Proceedings of the 19th National Conference on Superconductivity, Bronisławów, Poland, October 6–11, 2019

DFT+U Study of Stability and Electronic Properties of Antiferromagnetic States of $Sr_4V_2O_6Fe_2As_2$

Thi Ly Mai* and Vinh Hung Tran

W. Trzebiatowski Institute of Low Temperature and Structure Research, Polish Academy of Sciences, P.O. Box 1410, 50-422 Wrocław, Poland

Doi: 10.12693/APhysPolA.138.740 *e-mail: t.l.mai@intibs.pl

We examine the magnetic stability and electronic properties of $Sr_4V_2O_6Fe_2As_2$ in the antiferromagnetic order of V, including the A-type (A-AF) and the checkerboard-type (c-AF), within the LDA+U approximation. Contrary to other reports, our data disclose that A-AF is more stable than c-AF for J in the range of $1 \div 1.2$ eV and U between 7 and 8 eV; likewise c-AF is more stable for the (U, J) sets of J up to 0.2 eV and U in the range of $6 \div 8$ eV. There are numerous energy bands crossing the Fermi level in the c-AF phase, suggesting a strong inter-band scattering which affects the high T_c superconductivity. Particularly, the calculated band structures expose the formation of a Dirac cone. Besides, the Fermi surface in both phases shows the multi-sheets character consisting of several hole-like cylinders around Γ–Z and electron-like sheets at M and X points. The electron localization function study reveals that electrons are distributed in the high anisotropic frame and a large itinerant character of Fe 3d and V 3d dominantly favors the superconductivity in $Sr_4V_2O_6Fe_2As_2$.

topics: FeAs-based superconductors, electronic properties, strong correlation, Dirac cone

1. Introduction

$Sr_4V_2O_6Fe_2As_2$, first identified by Zhu et al. [1], is the highest critical temperature ($T_c \approx 37$ K) superconductor among $A_4M_2O_6Fe_2As_2$ (A = Ca, Sr, Ba and M = V, Cr, Sc) iron-based materials, the so-called 42622 [1, 2]. Similarly to other 42622 compounds, $Sr_4V_2O_6Fe_2As_2$ is built of thick perovskite blocks of Sr_2VO_3, alternated with FeAs layers in a long distance. As a consequence of the magnetic V ions, the physical properties occurrence in this superconductor can be more complicated than in other Fe-based materials. Until now, many theoretical [3–7] and experimental attempts [8–10] have been made with the aim to figure out the real magnetic behavior, the interaction between electrons (especially in V ions), as well as their effect on the high-T_c superconductivity. It is worth noting that by using the ^{57}Fe Mössbauer spectroscopy measurement Cao et al. [8] showed the nonmagnetic ordering of Fe. Besides, the antiferromagnetic arrangement in V sites was observed through the neutron-scattering measurement of Tegel et al. [9] and polarized neutron diffraction of Hummel et al. [10].

In the theoretical study aspects, the A-type (A-AF) and checkerboard anti-ferromagnetic (c-AF) ordering are found to be the most stable configurations of V among many considered magnetic cases [4, 7, 11, 12]. Recently, Nakamura et al. investigated the correlated behavior of vanadium electrons on c-AF phase $Sr_4V_2O_6Fe_2As_2$ using the LDA+U method for four sets of Hubbard U and Hund's coupling J parameters [12]. Their obtained results suggest that with the value of $U = 5$ eV or $U = 5.5$ eV, the blocking layer becomes insulating and the Fermi surface becomes quite similar to those in other iron-based superconductors. Although these efforts have exposed some special clues, many issues disclose a disagreement and therefore have not been completely clarified. Obviously, the influence of electrons correlation strength on the stability as well as the electronic properties of both A-AF and c-AF $Sr_4V_2O_6Fe_2As_2$ have not been investigated in detail. Therefore, in order to carefully determine the stable configuration under the influence of electrons correlation, we investigate the total energy of both the A-AF and c-AF arrangement in V sites and non-magnetic ordering in Fe sites as determined in experiment data for $Sr_4V_2O_6Fe_2As_2$, where the $U \sim (0 \div 8)$ and $J \sim (0 \div 1.2)$ are taken into account. Moreover, to study the electronic behavior upon the correlation effect, the comparison of electronic properties of the most stable state between two of these magnetic configurations is performed.

2. Computational details

$Sr_4V_2O_6Fe_2As_2$ superconductor crystallizes in the tetragonal structure with the space group $P4/nmm$ (No. 129) [1]. Based on our measurement results, the crystallographic data of this compound are the following: $a = b = 3.9318$ Å, $c = 15.6910$ Å,

$z_{\mathrm{Sr1}} = 0.1903$, $z_{\mathrm{Sr2}} = 0.4145$, $z_{\mathrm{V}} = 0.3081$, and also $z_{\mathrm{O1}} = 0.2922$, $z_{\mathrm{O2}} = 0.4318$, $z_{\mathrm{Fe}} = 0.0000$, $z_{\mathrm{As}} = 0.0909$. To fully perform the calculations of the antiferromagnetic ordering of V, A-AF (ions on the neighboring layers have opposite moments) and c-AF (the neighboring magnetic ions on the same layer have opposite moments) as presented in [12], the unit cell was expanded along *ab* plane to $\sqrt{2}a \times \sqrt{2}a \times 1c$ size containing 32 atoms. The whole calculation procedures were carried out using the LDA+U method implemented in the Vienna *ab initio* simulation package (VASP) [13], where the effective Hubbard U_{eff} and Hund's coupling J were taken into account. The Brillouin zone was used as $4 \times 4 \times 2$ Monkhorst–Pack grid including 220 k-points and the plane-wave energy cut-off was 400 eV. The self-consistent loops were finished when the different energy fell down by 5×10^{-5} eV and the force was under 0.01 eV/Å.

3. Results and discussion

To compare the stability of $Sr_4V_2O_6Fe_2As_2$ in the magnetic state upon the strong correlation effect of V electrons, in Fig. 1 we present the differences in energies between two antiferromagnetic configurations as the function of U and J. This comparison indicates that magnetic stabilities depend strongly on (U, J) values. It turns out that A-AF is more stable for J in the energy ranges $1.1 \div 1.2$ eV and U between 7 and 8 eV, while c-AF is more stable for the (U, J) sets of J up to 2 eV and $U = 7 \div 8$ eV. One important finding is that the calculated magnetic moment of V is 1.3 μ_{B}/V in A-AF and 1 μ_{B}/V in c-AF which is fairly smaller than those in other cases of (U, J) of Nakamura et al. results for the c-AF state [12], respectively. Otherwise, we have not found any magnetic arrangement in Fe sites that is similar to the observation in ^{57}Fe Mössbauer spectroscopy measurement of Cao et al. [8]. In the following, we investigate the electronic properties of $Sr_4V_2O_6Fe_2As_2$ with $U_{\mathrm{eff}} = U - J = 1$ eV, where $J = 1.2$ eV.

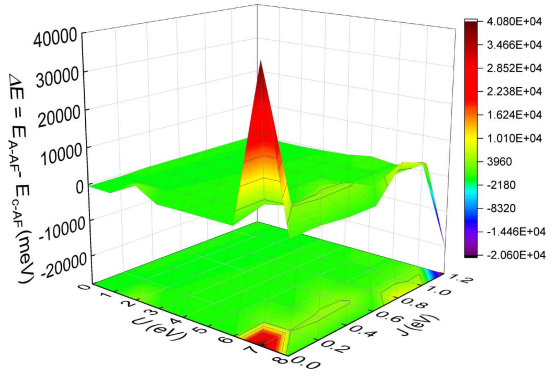

Fig. 1. Differences in total energies between two AF magnetic configurations as a function of U_{eff} and J.

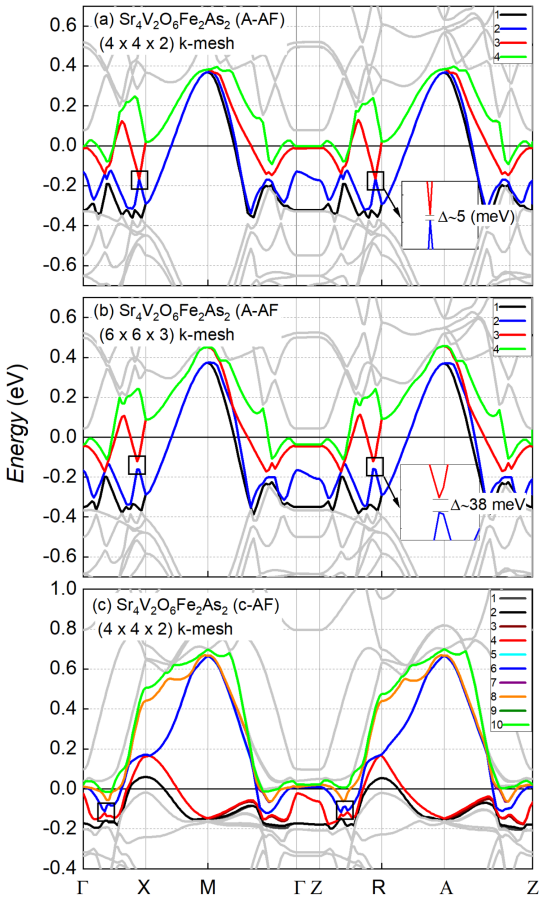

Fig. 2. Electronic band structures of A-AF in (a) $(4 \times 4 \times 2)$ k-mesh and (b) in $(6 \times 6 \times 3)$ k-mesh, and (c) c-AF in $(4 \times 4 \times 2)$ k-mesh of $Sr_4V_2O_6Fe_2As_2$.

The electronic band structures of two considered magnetic configurations of $Sr_4V_2O_6Fe_2As_2$ are demonstrated in Fig. 2, where the bands overpassing the Fermi level are presented in the color format. There are four bands crossing the Fermi level (E_{F}) in the A-AF state (Fig. 2a, b) and they increase to ten bands due to a slight split of bands around Γ–Z line in c-AF (Fig. 2c). A larger number of bands overpassing E_{F} in c-AF denotes a stronger inter-band scattering as compared to those in A-AF. It is recognized that bands 1 and 2, 3 and 4 in the A-AF phase seem to coincide with each other along X–M and R–A, suggesting a weak spin splitting (spin polarization) in the direction of the Brillouin zone. Besides, in the A-AF phase, the crossing bands form the electron-like pockets around M and A points but in the c-AF phase they form the electron-like pockets around X and R points. Moreover, the density of states (DOS) close to E_{F} in A-AF is dominantly contributed by bands 3 and 4, whereas bands 5 to 8 mainly contribute to the DOS around E_{F} in c-AF. Especially, bands 2 and 3 in A-AF and bands 4 and 5 in c-AF bend at some points near the Fermi level, noted in the black rectangle which forms the shape of a Dirac cone separated by a small gap. The width

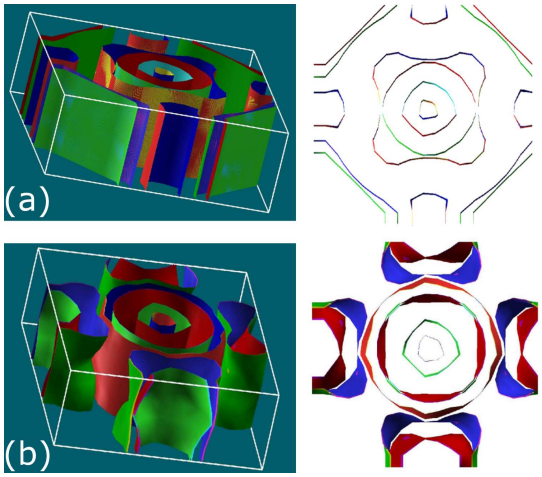

Fig. 3. Fermi surfaces in 3D and the 2D-quasi configuration of (a) A-AF and (b) c-AF $Sr_4V_2O_6Fe_2As_2$.

of this gap depends on the change of input parameters such as k-mesh size, Hubbard U, Hund's coupling J or cut-off energy value (ENMAX), etc. In the case of $(U_{\text{eff}}, J) = (1, 1.2)$ eV, $4\times4\times2$ k-mesh with ENMAX= 400 eV, the energy gap is around 5 meV (as shown in Fig. 2a). Otherwise, that becomes larger than 13 meV when $U_{\text{eff}} = 5$ eV, 15 meV when ENMAX = 500 eV or up to 38 meV when the $6 \times 6 \times 3$ k-mesh size is chosen (see Fig. 2b). It is necessary to note here that the same observations of a Dirac cone have been made for other iron-based superconductors [14, 15]. Therefore, further measurements are encouraged to examine $Sr_4V_2O_6Fe_2As_2$.

The 3D and 001-configuration Fermi surfaces (FS) topologies of $Sr_4V_2O_6Fe_2As_2$ in both the A-AF and c-AF phases are depicted in Fig. 3. Obviously, the FS shows a multi-sheets character containing several hole-type cylinders around the Brillouin zone center formed by band numbers 3 and 4 in A-AF or band numbers 5 to 10 in c-AF. Moreover, we found that there are two electron-type sheets coming from bands 1 and 2 at the corner of the Brillouin zone (M point) and another one from band 3 at X point in the A-AF state. Otherwise, in c-AF all of electron-type sheets from bands $1 \div 4$ locate around X point. Generally, the FS dispersion in c-AF is mostly larger than the dispersion in the A-AF configuration. Patently, the difference in the FS between the two phases is related to the change of magnetic arrangement of V.

In order to examine the nature of atomic bonding and its character, the electron localization function (ELF) of $Sr_4V_2O_6Fe_2As_2$ is also investigated. Figure 4 shows the 3D visualization and iso-surfaces cutting in some special planes in which the ELF values of 0 and 1 correspond to the perfect delocalization and localization of electrons. Generally, ELF maps reveal the dramatic change of value suggesting a high anisotropy distribution of

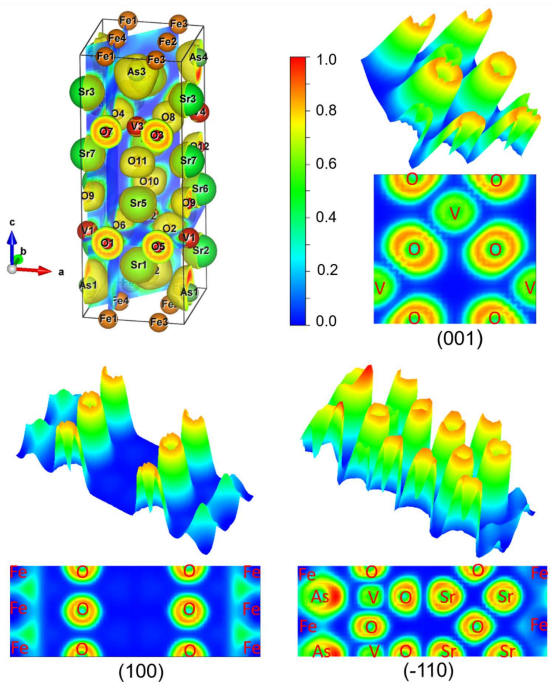

Fig. 4. 3D visualizations of crystal supercell and the ELF iso-surface cutting in the (001)-, (100)-, (−110)-plane of $Sr_4V_2O_6Fe_2As_2$.

electrons. The highest ELF value of 0.9 is found in As sites (shown in −110 iso-surface) or 0.8 in Sr, O sites (shown in 001, 100, −110 iso-surface), indicating that the electrons are mostly localized around these atoms. The ELF approximating 0.5 in the V atoms (shown in 001 and −110 iso-surface) or even 0.1 in Fe ones (shown in 100, −110 iso-surface) reveal the delocalization of electrons. Obviously, the itinerant behaviors of Fe 3d and V 3d electrons, where Fe plays a dominant role, assist the superconductivity.

4. Conclusions

We have investigated the dependence of the total energy of the A-type antiferromagnetic (A-AF) and the checkerboard-antiferromagnetic (c-AF) $Sr_4V_2O_6Fe_2As_2$ on the effect of electrons correlation of V using the LDA+U method. The total energy comparison between the two considered magnetic phases indicates that A-AF is more stable than c-AF for $U_{\text{eff}} > 7$ eV and $J > 1.2$ eV, whereas c-AF is more stable for $U_{\text{eff}} \approx 8$ eV and $J < 0.2$ eV. In both AF cases, there are numerous bands crossing the Fermi energy, suggesting strong inter-band scattering. Especially, the bands exhibit a Dirac-cone shape near the Fermi level which calls for a further experimental confirmation. The Fermi surface is characterized by several hole-type cylinders at the Γ point and electron-type sheets around M in the A-AF state or around X point in c-AF. Additionally, the ELF map reveals a high anisotropy of electrons' distribution. Furthermore, a low ELF

value in Fe and V sites suggests the itinerant character of their electrons. These Fe $3d$ and V $3d$ electrons are responsible for the superconductivity of $Sr_4V_2O_6Fe_2As_2$.

Acknowledgments

The financial support by the National Science Centre of Poland under the grant No. 2016/21/B/ST3/01366 is gratefully acknowledged.

References

[1] X. Zhu, F. Han, G. Mu, P. Cheng, B. Shen, B. Zeng, H.-H. Wen, *Phys. Rev. B* **79**, 220 (2009).

[2] H. Ogino, S. Sato, Y. Matsumura, N. Kawaguchi, K. Ushiyama, Y. Katsura, S. Horii, K. Kishio, J. Shimoyama, *Phys. C Supercond.* **470**, 280 (2010).

[3] K.-W. Lee, W.E. Pickett, *Europhys. Lett.* **89**, 57008 (2010).

[4] I.I. Mazin, *Phys. Rev. B* **81**, 020507 (2010).

[5] T. Qian, N. Xu, Y.B. Shi et al., arXiv:1008.4905 (2010).

[6] I.R. Shein, A.L. Ivanovskii, *J. Supercond. Novel Magn.* **22**, 613 (2009).

[7] G. Wang, M. Zhang, L. Zheng, Z. Yang, *Phys. Rev. B* **80**, 184501 (2009).

[8] G.-H. Cao, Z. Ma, C. Wang, et al., *Phys. Rev. B* **82**, 104518 (2010).

[9] M. Tegel, T. Schmid, T. Stürzer, M. Egawa, Y. Su, A. Senyshyn, D. Johrendt,*Phys. Rev. B* **82**, 140507(R) (2010).

[10] F. Hummel, Y. Su, A. Senyshyn, D. Johrendt, *Phys. Rev. B* **88**, 144517 (2013).

[11] Y. Tojo, T. Shibuya, T. Nakamura et al., *J. Condens. Matter Phys.* **31**, (2019).

[12] H. Nakamura, M. Machida, *Phys. Rev. B* **82**, 094503 (2010).

[13] G. Kresse, J. Hafner, *Phys. Rev. B* **47**, 558 (1993).

[14] P. Richard, K. Nakayama, T. Sato et al., *Phys. Rev. Lett.* **104**, 1079 (2010).

[15] Z.T. Liu, X.Z. Xing, M.Y. Li et al., *Appl. Phys. Lett.* **109**, 042602 (2016).